

# StableMaterials: Enhancing Diversity in Material Generation via Knowledge Distillation and Semi-Supervised Learning

GIUSEPPE VECCHIO, Independent Researcher, Italy



Fig. 1. We present StableMaterials, a diffusion-based model for materials generation through text or image prompting. Our approach enables high-resolution, tileable material maps, inferring both diffuse (Basecolor) and specular (Roughness, Metallic) properties, as well as the material mesostructure (Height, Normal).

We introduce **StableMaterials**, a novel approach for generating photorealistic physical-based rendering (PBR) materials that integrate semi-supervised learning with Latent Diffusion Models (LDMs). Our method employs adversarial training to distill knowledge from existing large-scale image generation models, minimizing the reliance on annotated data and enhancing the diversity in generation. This distillation approach aligns the distribution of the generated materials with that of image textures from an SDXL model, enabling the generation of novel materials that are not present in the initial training dataset. Furthermore, we employ a diffusion-based refiner model to improve the visual quality of the samples and achieve high-resolution generation. Finally, we distill a latent consistency model for fast generation in just four steps and propose a new tileability technique that removes visual artifacts typically associated with fewer diffusion steps.

We detail the architecture and training process of StableMaterials, the integration of semi-supervised training within existing LDM frameworks, and show the advantages of our approach. Comparative evaluations with state-of-the-art methods show the effectiveness of StableMaterials, highlighting its potential applications in computer graphics and beyond. StableMaterials is publicly available at <https://gvecchio.com/stablematerials>.

CCS Concepts: • **Computing methodologies** → **Computer graphics**.

Additional Key Words and Phrases: material appearance, generative models

Author’s address: Giuseppe Vecchio, Independent Researcher, Italy, [giuseppevecchio@hotmail.com](mailto:giuseppevecchio@hotmail.com).

## 1 INTRODUCTION

Authoring of materials has been a long-standing challenge in computer graphics, requiring very specialized skills and a high level of expertise. To simplify the creation of materials for 3D applications, such as videogames, architecture design, simulation, media, and more, recent methods have tried to leverage learning-based approaches to capture materials from input images [Bi et al. 2020; Deschaintre et al. 2018, 2019; Gao et al. 2019; Guo et al. 2021; Li et al. 2017, 2018; Martin et al. 2022; Vecchio et al. 2023, 2021; Zhou and Kalantari 2021], or generation from a set of conditions [Guehl et al. 2020; Guo et al. 2020; He et al. 2023; Hu et al. 2022; Vecchio et al. 2023, 2024; Zhou et al. 2022]. While these approaches have reduced technical barriers to material creation, their effectiveness depends on the quality and diversity of training data, which can limit their use in real-world applications.

Despite recent efforts to create large-scale materials datasets, such as Deschaintre et al. [2018], OpenSVBRDF [Ma et al. 2023], and MatSynth [Vecchio and Deschaintre 2024], these datasets are limited in diversity [Zhou et al. 2023], not capturing the vast range observed in large-scale image datasets such as LAION [Schuhmann et al. 2022]. These limitations can constrain the capabilities of learning-based approaches, potentially creating gaps in their generative capabilities and affecting realism and diversity.

Fine-tuning has become a common practice to reduce these gaps in training data by leveraging existing knowledge from large-scale pretrained models. Techniques like Low-Rank Adaptation (LoRA) [Hu et al. 2021] effectively fine-tune models while preventing catastrophic forgetting. Methods such as Diff-Instruct [Luo et al. 2024], on the other hand, employ distillation strategies to transfer knowledge from pretrained models. However, while fine-tuning or distillation within the same domain are straightforward, they pose significant challenges across different domains (e.g., image to material).

To overcome these limitations, we introduce **StableMaterials**, an approach that takes advantage of semi-supervised adversarial training to: (1) include unannotated (non-PBR) samples in training, and (2) distill knowledge from a large-scale pretrained SDXL [Podell et al. 2023] model. In particular, we use a pretrained SDXL to generate unannotated texture samples from text prompts. However, since StableMaterials is trained to produce SVBRDF maps, we cannot perform direct supervision using the generated textures. To include these textures in the training of our methods, we learn a common latent representation between textures and materials; then, we complement the traditional supervised loss, with an unsupervised adversarial loss, forcing the model to also generate realistic maps for unannotated samples and close the gap between the two data distributions. In addition, drawing inspiration from the SDXL [Podell et al. 2023] architecture, we use a diffusion-based refinement model to enhance the visual quality of the samples and achieve high-resolution generation. We initially generate materials at the model base resolution of 512x512, and subsequently apply our refiner using SDEdit [Meng et al. 2021] and patched diffusion. This approach allows to achieve high resolution while constraining the patched generation, ensuring consistency and memory efficiency. Subsequently, we distill a latent consistency model [Song et al. 2023] that allows fast generation by reducing the number of inference steps to four steps per stage. However, this comes at the cost of introducing visible seams when using approaches such as *noise rolling* [Vecchio et al. 2023] to achieve tileability. To solve this issue, we propose a novel *features rolling* technique, which shifts the tensor rolling from the diffusion step to the U-Net architecture by directly shifting the feature maps within each convolutional and attention layer.

We qualitatively evaluate our method and compare it with previous work, demonstrating the benefit of our semi-supervised training approach. In summary, we introduce StableMaterials a novel solution combining supervised and adversarial training to generate highly realistic material in scenarios where annotated data are scarce. The contributions of this work are as follows:

- StableMaterials, a new diffusion-based model for PBR material generation, leveraging a semi-supervised learning approach to incorporate unannotated data during training.
- A novel distillation technique to bridge the gap with large-scale models by including unannotated data in the training.
- A novel “features rolling” approach to tileability, minimizing the visual artifacts produced by fewer diffusion steps.
- State-of-the-art performance in PBR materials generation.

## 2 RELATED WORK

**Materials Generation.** Materials synthesis is an open challenge in computer graphics [Guarnera et al. 2016] with many recent data-driven approaches focusing on estimating SVBRDF maps from an image [Bi et al. 2020; Deschaintre et al. 2018, 2019; Gao et al. 2019; Guo et al. 2021; Li et al. 2017, 2018; Martin et al. 2022; Vecchio et al. 2023, 2021; Zhou and Kalantari 2021]. Building on the success of generative models, several approaches to materials generation have emerged, including Guehl et al. [2020] which combines procedural structure generation with data-driven color synthesis; MaterialGAN [Guo et al. 2020], a generative network which produces realistic SVBRDF parameter maps using the latent features learned from a StyleGAN2 [Karras et al. 2020a]; Hu et al. [2022] which generates new materials transferring the micro and meso-structure of a texture to a set of input material maps; and TileGen [Zhou et al. 2022], a generative model capable of producing tileable materials, conditioned by an input pattern but limited to class-specific training. Recent approaches have focused on leveraging the generative capabilities of diffusion models for materials generation. In particular, Vecchio et al. [2023] introduced ControlMat, which relies on the MatGen diffusion backbone, to capture materials from an input image. MatFuse [Vecchio et al. 2024] extends generation control with multimodal conditioning, and enables editing of existing materials via ‘volumetric’ inpainting. MaterialPalette [Lopes et al. 2024] extends the capture of materials to pictures of real-world scenes by finetuning a LoRA [Hu et al. 2021] for each picture. Substance 3D Sampler [Adobe 2024] recently introduced a pipeline to generate materials by first synthesizing a texture via text conditioning. However, these methods often lack diversity, struggling with complex material representation, or depend on image generation models, requiring additional steps to estimate the material parameters. StableMaterials overcomes these limitations by including a wider variety of unannotated material samples via a semi-supervised training and improves on inference time by distilling a latent consistency model.

**Generative models.** Image generation is a long-standing challenge in computer vision, primarily due to the high dimensionality of images and complex data distributions. Generative Adversarial Networks (GAN) [Goodfellow et al. 2014] enabled the creation of high-quality images [Brock et al. 2018; Karras et al. 2017, 2020b], yet they suffer from unstable training [Arjovsky et al. 2017; Gulrajani et al. 2017; Mescheder 2018], leading to mode collapse behaviour.

Diffusion Models (DMs) [Ho et al. 2020; Sohl-Dickstein et al. 2015], particularly the more efficient Latent Diffusion (LDM) architecture [Rombach et al. 2022], have emerged as an alternative to GANs, achieving state-of-the-art results in image generation tasks [Dhariwal and Nichol 2021], besides showing a more stable training. Following the success of LDMs, research has focused on improving the generation quality [Podell et al. 2023] and reducing the number of inference steps to speed up the generation process [Luo et al. 2023; Sauer et al. 2024, 2023b; Song et al. 2023] through model distillation. Furthermore, due to the proliferation of large-scale pretrained models, several approaches were proposed to reuse their knowledge [Hu et al. 2021; Luo et al. 2024; Ruiz et al. 2023]. However, these approaches focus on fine-tuning within the same image domain, restricting their applicability to non-image domains.

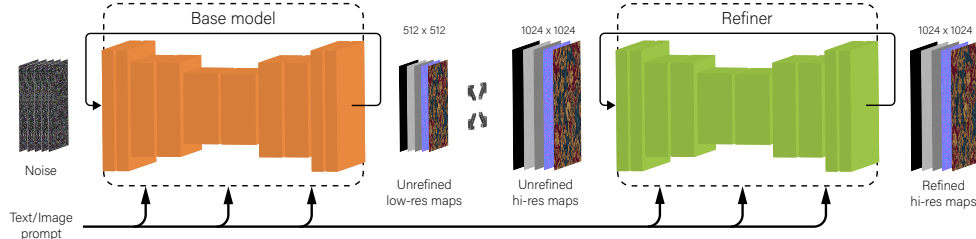


Fig. 2. **Architecture of StableMaterials.** The *base model* generates a low resolution materials of size 512x512. This generation is then upscaled and refined using SDEdit [Meng et al. 2021] by the *refiner model* using a patched approach to limit memory requirements.

### 3 METHOD

StableMaterials’ architecture, shown in Fig. 2, is based on MatFuse [Vecchio et al. 2024], which adapts the LDM paradigm [Rombach et al. 2022] to synthesize high-quality pixel-level reflectance properties for arbitrary materials. We modify the original MatFuse architecture, which employed a multi-encoder VAE to learn a disentangled latent representation of the maps, by fine-tuning a resource-efficient single-encoder compression model with the same latent properties. Additionally, we introduce a semi-supervised training strategy to distill knowledge from a large-scale SDXL model and improve generation diversity. We employ latent consistency distillation [Song et al. 2023] and a novel *feature rolling* technique for fast tileble generation, and achieve high resolution via a *refiner model*.

#### 3.1 Material Representation

StableMaterials generates materials in the form of SVBRDF texture maps, representing a spatially varying Cook-Torrance microfacet model [Cook and Torrance 1982; Karis 2013], using a GGX [Walter et al. 2007] distribution function, as well as the material mesostructure. In particular, we generate *base color*, *normal*, *height*, *roughness* and *metalness* properties, with the roughness determining the BRDF specular lobe width and the metalness defining which area of the material represents a conductor.

#### 3.2 Material Generation

The generative model consists of a compression VAE [Kingma and Welling 2013]  $\mathcal{E}$ , encoding the material maps into a compact latent space, and a diffusion model [Rombach et al. 2022]  $\epsilon_\theta$ , modeling the distribution of these latent features.

*Map Compression.* We first train a multi-encoder VAE, consisting of a set of encoders  $\mathcal{E} = \{\mathcal{E}_1, \mathcal{E}_2, \dots, \mathcal{E}_N\}$  and a decoder  $\mathcal{D}$ , to encode  $N$  material maps  $M = \{\mathbf{M}_1, \mathbf{M}_2, \dots, \mathbf{M}_N\}$  into their latent representation  $z = \text{concat}(z_1, z_2, \dots, z_N)$ , with  $z_i = \mathcal{E}_i(\mathbf{M}_i)$  being the encoding of the  $i^{\text{th}}$  map using the  $i^{\text{th}}$  encoder  $\mathcal{E}_i$ .

The latent tensor  $z$  is then decoded to reconstruct the input maps  $\hat{M} = \mathcal{D}(z)$ . Following [Vecchio et al. 2024], the VAE is trained using pixel-space  $L_2$  loss, perceptual LPIPS loss [Zhang et al. 2021], a patch-based adversarial objective [Dosovitskiy and Brox 2016; Isola et al. 2017], and a rendering loss [Deschaintre et al. 2018]. We regularize the VAE latent space using a Kullback-Leibler divergence penalty [Kingma and Welling 2013; Rezende et al. 2014].

Following the training of the multienncoder VAE, we fine-tune a resource-efficient single encoder model. In particular, we freeze

the decoder and train only the maps encoder  $\mathcal{E}'$  to compress the concatenated material maps to the same latent representation  $z$ . This encoder maintains the original’s disentangled latent representation and compression efficiency with fewer parameters. We compare the two models in Sec. 4.4.1.

Finally, we learn a common latent representation between texture images and materials, allowing us to incorporate these unannotated textures into the training process. To do so, we fine-tune an autoencoder model to compress a single texture (i.e.: the basecolor map) into  $z$ . Similarly to the single-encoder model, we keep the decoder frozen and train the encoder only. This network is used for semi-supervised training, allowing us to inject unannotated textures generated using SDXL in the training. We detail the use of this model in Sec. 3.3.

*Diffusion Model.* We train a diffusion model on a compressed latent representation  $z$  of the material. This model, based on the architecture of Rombach et al. [2022], uses a time-conditional U-Net [Ronneberger et al. 2015] to denoise the latent vectors  $z$ . During training, we generate noised latent vectors using a deterministic forward diffusion process  $q(z_t|z_{t-1})$ , as defined in Ho et al. [2020], transforming them into an isotropic Gaussian distribution. The diffusion network  $\epsilon_\theta$  learns the backward diffusion  $q(z_{t-1}|z_t)$  to denoise and reconstruct the original latent vector. The model training is described in Sec. 3.3

*Conditioning.* StableMaterials enables control over the generation via high-level text or image prompts, descriptive of the global appearance of the material. Conditions are encoded into a one-dimensional feature vector using a pretrained CLIP [Radford et al. 2021] model. During training, we alternate between images and text prompts to enhance the robustness of the model. In particular, we use an ambient-lit rendering of the material as the image condition and the caption as text prompt. For materials without a caption, we use descriptive tags to build a text prompt. For each training batch, we select between image and text conditioning modes by randomly dropping one modality. A drop probability of 75% for text and 25% for image empirically proved to be the most effective.

#### 3.3 Semi-Supervised Adversarial Distillation

To reduce the gap with image generation methods trained on large-scale datasets, we propose to distill knowledge from an SDXL model. However, direct distillation is impractical due to domain differences

between textures, represented from a single image, and materials, represented by multiple maps; therefore, we propose a semi-supervised approach to include unannotated samples (i.e.: textures without explicit material properties representation) during training. In particular, we complement the *supervised* loss with an *unsupervised* adversarial loss through a discriminator on the latent space (*LD*). This adversarial loss forces the generator to synthesize materials that present features similar to ground-truth ones, while the discriminator learns to distinguish between the two data sources. The generator is trained using samples from the material dataset as well as unannotated textures, while the discriminator is trained using only annotated samples.

Our generator is optimized using a combination of supervised and adversarial losses. The supervised loss,  $\mathcal{L}_{\text{sup}}$ , is defined as:

$$\mathcal{L}_{\text{sup}} = \mathbb{E}_{z_t, z_0, \epsilon} \left[ \left\| \epsilon_t, \epsilon_\theta(z_t, \text{mat}, t) \right\|^2 \right] + \alpha \mathbb{E}_{z_t, z_0, \epsilon} \left[ \left\| \epsilon_t, \epsilon_\theta(z_t, \text{tex}, t) \right\|^2 \right] \quad (1)$$

comparing the model-estimated noise  $\epsilon_\theta(z_t, t)$  with the actual noise  $\epsilon_t$  introduced during the forward diffusion process [Ho et al. 2020]. Here,  $z_{t, \text{mat}}$  and  $z_{t, \text{tex}}$  are the noisy latent at timestep  $t$  for the materials and textures samples respectively. The loss computed on unannotated texture samples is weighted using the hyperparameter  $\alpha$ , set to 0.15 in our experiments.

The adversarial objective  $\mathcal{L}_{\text{adv}}$  push the generator to close the distribution gap between materials and textures, producing outputs that are perceived as materials by the discriminator. It is computed on the denoised latents at timestep  $t - 1$ , and is defined as:

$$\mathcal{L}_{\text{adv}} = -\mathbb{E}_{z \sim p(z)} [LD(z_{t-1})] \quad (2)$$

with  $z_{t-1} = \text{concat}(z_{t-1, \text{mat}}, z_{t-1, \text{tex}})$  the concatenated denoised latents and  $LD(\cdot)$  the output of the latent discriminator.

Following Sauer et al. [2021, 2023a], *LD* is trained using a hinge loss function [Lim and Ye 2017] computed between the noised latent embeddings of the materials  $z_{t-1, \text{real}}$  encoded with the VAE, and  $z_{t-1, \text{fake}}$  the denoised latents from the generator.

*LD* shares the same architecture as the conditional diffusion U-Net encoder and is initialized with the weights of the diffusion U-Net. Functioning in a time-conditional manner, it incorporates the diffusion timestep and the CLIP embeddings from either text or image prompts, ensuring that evaluations are relevant to the desired material appearance.

### 3.4 Fast High-Resolution Generation

*Few steps generation.* To enhance generation efficiency, we fine-tune a Latent Consistency Model [Luo et al. 2023] (LCM). This model streamlines the denoising process by implementing a one-stage guided distillation of an augmented probability flow ordinary differential equation (PF-ODE). The distillation leverages a consistency function  $f_\theta : (z_t, c, t) \mapsto z_0$ , which directly predicts the PF-ODE solution at  $t = 0$ . Compared to two-stage methods [Meng et al. 2023], LCM integrates the guidance scale  $\omega$  directly into the augmented PF-ODE. Additionally, LCM adopts a skipping step strategy, ensuring consistency not between consecutive steps, but between steps separated by  $k$ , thus  $t_{n+k} \rightarrow t_n$ , circumventing alignment issues in traditional models. The use of consistency models enables few-steps generation, resulting in fast material synthesis as detailed in Sec. 4.2.

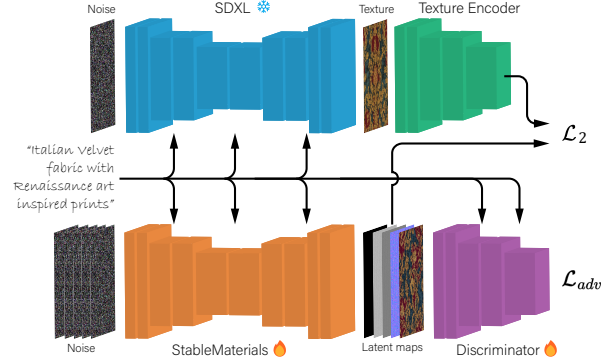


Fig. 3. **Semi-Supervised training.** Both the SDXL model and StableMaterials are prompted to generate the same material. The supervised  $\mathcal{L}_2$  loss is complemented by an adversarial loss  $\mathcal{L}_{\text{adv}}$  computed on the denoised latent from StableMaterials.

*Features rolling.* Recent material generation methods achieve tileability via *noise rolling* [Vecchio et al. 2023], leveraging the iterative nature of diffusion models. However, this approach becomes ineffective with fewer generation steps, being unable to fully remove seams. Circular padding [Zhou et al. 2022], on the other hand, despite being independent of diffusion steps, is not suitable for patched generation as it causes self-tileability in patches.

To address these issues, we propose shifting tensor rolling from the diffusion step to the U-Net architecture by directly rolling the feature maps. This method, named *features rolling*, integrates rolling within U-Net blocks, reducing the need for multiple diffusion steps. By randomly translating and then reversing feature maps within each convolution and attention layer in the U-Net, this approach preserves edge continuity and minimizes visual artifacts typically associated with fewer diffusion steps. To better preserve structure in highly structured materials, we enable *features rolling* after the first diffusion step. We compare *features rolling* with other approaches to tileability in the Supplemental Materials.

*Latent Upscaling & Refinement.* Features rolling in combination with patch diffusion allows efficient high-resolution generation; however, it results in inconsistent generations between patches, due to the loss of cross-patch dependencies.

To overcome this limitation, we use a two-stage pipeline, similar to the one introduced in SDXL [Podell et al. 2023], where the output of the base model is further refined by a high-resolution expert using SDEdit [Meng et al. 2021]. This approach allows us to use patched diffusion in the refinement process while keeping the overall content consistent with the original generation. In particular, we first generate at the model’s base 512x512 resolution, and then refine it at the desired resolution. We apply the SDEdit refinement with a strength of 0.5, which we find to be the best compromise between new high-frequency details creation and consistency with the previous step generation. To better learn the high-frequency features of the materials, the refiner model is trained on 512x512 crops extracted from the 4K materials at their full resolution without downsampling. We show the quality improvement of this approach in the ablation study, Sec. 4.4.3, and provide additional samples in Supplemental Materials.

## 4 IMPLEMENTATION & RESULTS

In this section, we first introduce the datasets used in our work, we then assess the generation capabilities of StableMaterials and compare it with recent state-of-the-art methods. Finally, we evaluate our design choices in the ablation studies.

### 4.1 Dataset

We train our model on the combined MatSynth [Vecchio and Deschaintre 2024] and Deschaintre et al. [2018] datasets, for a total of 6, 198 unique PBR materials, using the original training/test splits. Our dataset includes 5 material maps (Basecolor, Normal, Height, Roughness, Metallic) and their renderings under different environmental illuminations. We complement the dataset with 4, 000 texture-text pairs from SDXL [Podell et al. 2023], using 200 prompts. We query a ChatGPT [OpenAI 2024] model to suggest relevant material prompts. The full list of prompts used, as well as samples generated from SDXL, are provided in the Supplemental Material.

### 4.2 Technical details

We train all models on a single NVIDIA RTX4090 GPU with 24GB of VRAM, employing gradient accumulation to achieve a larger batch.

*Autoencoder.* The compression model is trained with mini-batch gradient descent, using the Adam optimizer [Kingma and Ba 2014] and a batch size of 8. We train the model for 1, 000, 000 iterations with a learning rate of  $4.5 \cdot 10^{-4}$  and enable the  $\mathcal{L}_{adv}$  after 300, 000 iterations as in Esser et al. [2021]. We first train a multi-encoder VAE [Vecchio et al. 2024]; then we fine-tune a single-encoder model to compress the concatenated maps into the same disentangled latent space, reducing the total of parameters from 271M to 101M, while keeping similar reconstruction performance (Tab. 1). We fine-tune both the single encoder model and the texture encoder for 100, 000 steps while keeping the decoder frozen.

*Latent Diffusion model.* The diffusion model is trained supervisedly for 400, 000 iterations with a batch size of 16 using an AdamW [Loshchilov and Hutter 2017] optimizer, with a learning rate of  $3.2 \cdot 10^{-5}$ . The model is fine-tuned semi-supervisedly for 200, 000 iterations with a batch size of 8. We fine-tune the refiner model for 50, 000 iterations using a batch size of 16 and a learning rate of  $2 \cdot 10^{-7}$ . Both models use the original OpenAI U-Net architecture with 18 input and output channels.

*Latent Consistency model.* The latent consistency model [Luo et al. 2023] is fine-tuned for 10, 000 iterations, with a batch size of 16, using an AdamW optimizer, with a learning rate value of  $1 \cdot 10^{-6}$ . We use a linear schedule for  $\beta$  and denoise using the LCM (Latent Consistency Models) sampling schedule at inference time with  $T = 4$  steps.

*Inference.* We assess execution speed and memory usage. We generate with 4 denoising steps, followed by 2 refinement steps, using the LCM sampler with a fixed seed and processing up to 8 patches in parallel. Both base and refiner models run at half-precision. Generation takes 0.6s at  $512 \times 512$ , 1.5s at  $1024 \times 1024$  and 6.5GB of VRAM, 4.9s at  $2048 \times 2048$  and 7.4GB VRAM, and 18.6s at  $4096 \times 4096$  and 12GB of VRAM. For comparison, the LDM with a

DDIM sampler and 50 generation steps, followed by 25 refinement steps, takes 20.6s at  $2048 \times 2048$ , and 65.4s at  $4096 \times 4096$ .

### 4.3 Results and comparison

For all results, we show generated material maps, as well as the rendering under ambient lighting. We include a wider variety results in the Supplemental Material, as well as material editing samples and a CLIP-based Nearest-Neighbour search in the training database.

*Generation results.* We evaluate our model generation capabilities for both image (Fig. 4 and Fig. 12) and text (Fig. 5 and Fig. 13) conditioning. The results show the ability of StableMaterials to closely follow the input prompt, producing diverse realistic materials. For each set of results, we show two *in-domain* generations, that is materials categories that are present in our annotated training dataset, and two *out-domain* samples, materials from the unannotated data, confirming the ability of StableMaterials to generate new high-quality materials from both data distributions.

*Comparison.* We compare StableMaterials against MatFuse [Vecchio et al. 2024] trained on MatSynth [Vecchio and Deschaintre 2024], MatGen<sup>1</sup> [Vecchio et al. 2023], Material Palette [Lopes et al. 2024], and the text-to-texture-to-material pipeline in Adobe Substance 3D Sampler [Adobe 2024]. Figures 6 and 7 show the generation results for image and text conditioning, respectively. It should be noted that MatFuse, Material Palette, and StableMaterials are trained on public datasets, while both MatGen and Sampler use private data. Furthermore, MatFuse, MatGen, and StableMaterials directly produce PBR maps, while MaterialPalette and Sampler employ a two-step process: first, generating a texture, then using an SVBRDF estimator to predict the material maps. This approach benefits from leveraging large image models, but suffers from biases inherent in SVBRDF predictions, which guess material properties from light-surface interactions, that are further exacerbated by the non-material-specific training sometimes generating natural images (with perspective) instead of surfaces. Moreover, MaterialPalette fine-tunes a LoRA for each prompt, introducing a time and computation overhead. In contrast, StableMaterials directly creates material maps by having learned material features, leading to more precise and unbiased results. MatFuse is constrained by its  $256 \times 256$  resolution, resulting in blurry, undetailed generations, and struggles with complex materials. MatGen, on the other hand, generally synthesizes high-quality materials, but presents oversharpener artifacts and struggles in following more complex prompts. We only show the generation renderings in Figures 6 and 7, with the PBR maps and additional samples included in the Supplemental Materials.

### 4.4 Ablation Study

We evaluate our different design choices by comparing the performance of our model against the baseline solutions. We provide high-resolution ablation results in the Supplemental Materials.

*4.4.1 VAE Architecture.* We report the reconstruction performance, in terms of RMSE, for both the multi-encoder and single-encoder models in Tab. 1. Results show that the adopted transfer-learning

<sup>1</sup>Generation samples for MatGen were kindly provided by the authors.

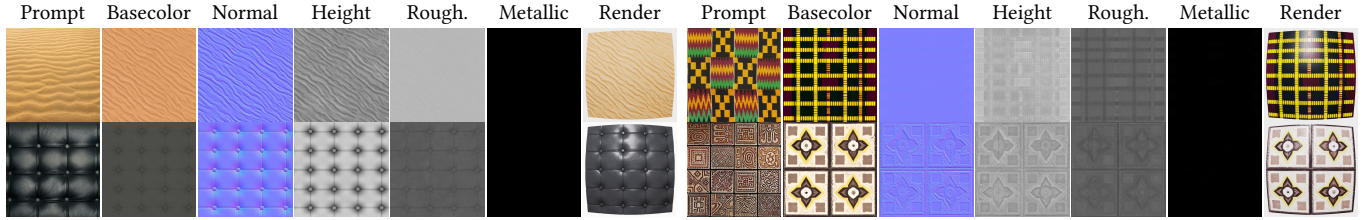


Fig. 4. **Image-prompting.** StableMaterials accurately captures the visual appearance of the input image, producing realistic materials for both in-domain (on the left) and out-domain (on the right) prompts. The render highlights the model’s ability to handle diverse and complex surfaces.

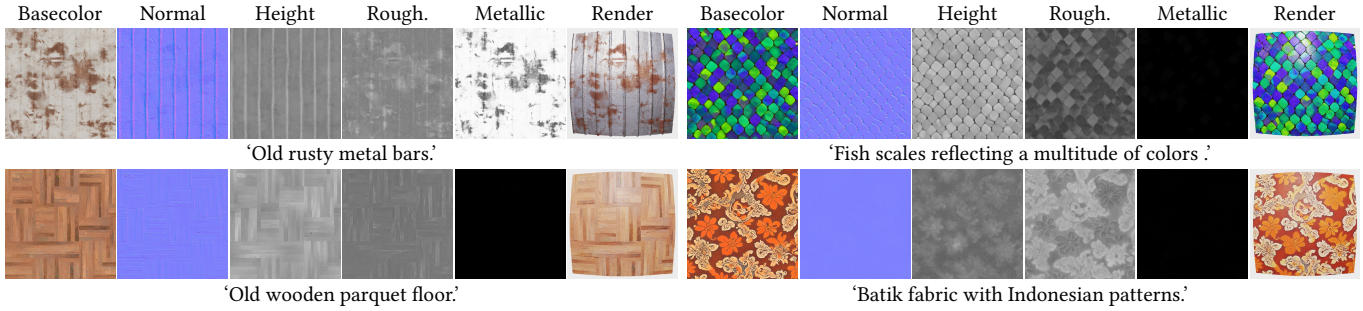


Fig. 5. **Text-prompting.** StableMaterials closely follow the input prompt, producing realistic materials for both in-domain (on the left) and out-domain (on the right) samples. The render highlights the model’s ability to generate accurate properties for different types of materials.

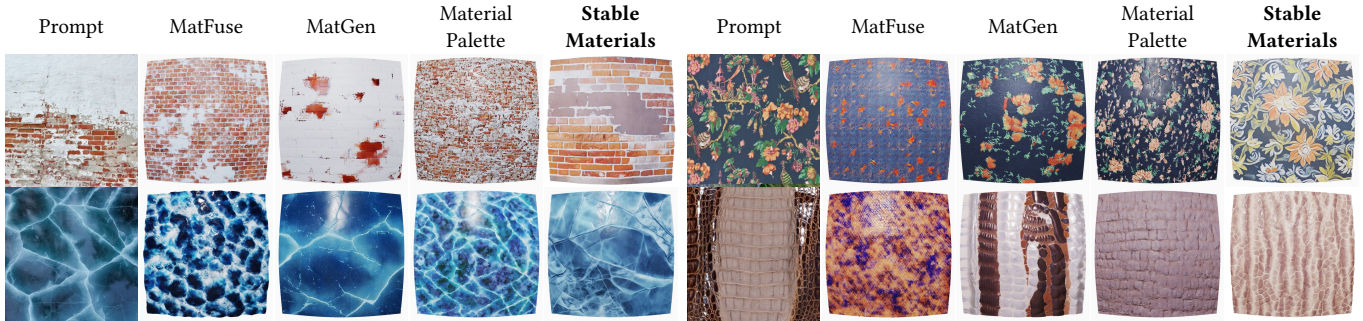


Fig. 6. **Comparison for image-prompting.** We compare StableMaterials with MatFuse, MatGen, and MaterialPalette in image-prompted generation, showing two in-domain (left column) and two out-domain (right column) renderings per model. StableMaterials improves over previous methods quality and ability to captures the visual appearance of the input image. Full set of maps in Supplemental Materials.

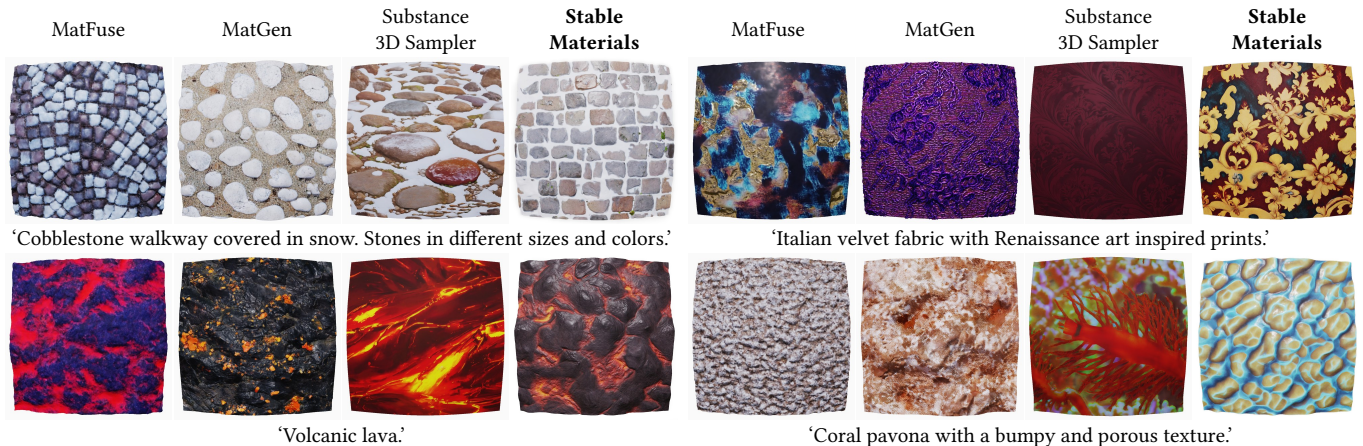


Fig. 7. **Comparison for text prompting.** We compare StableMaterials with MatFuse, MatGen, and Substance 3D Sampler on text-prompted generation, showing two in-domain (left column) and two out-domain (right column) renderings per model. StableMaterials better follows the input prompt and successfully models out-domain materials. Visual quality is on par or better than models trained on larger datasets. Full set of maps in Supplemental Materials.

Table 1. **Analysis of the VAE architecture.** We report the RMSE↓ between reconstructed and ground-truth maps. The single-encoder model, although having less parameters, achieves performances on par with the multi-encoder VAE.

	Basecolor	Normal	Height	Rough.	Metallic
Multi- $\mathcal{E}$ (271M par.)	0.030	<b>0.035</b>	<b>0.030</b>	<b>0.032</b>	0.016
Single- $\mathcal{E}$ (101M par.)	<b>0.028</b>	0.037	<b>0.030</b>	<b>0.032</b>	<b>0.015</b>

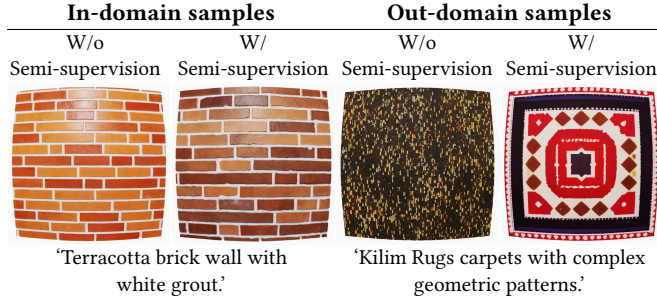


Fig. 8. **Ablation study of the training strategies.** The model effectively generates high-quality material with image or text prompts but struggles with unrepresented materials. Semi-supervised learning improves generation quality and diversity, including new materials.



Fig. 9. **Refinement ablation results.** Generation crops: the use of a diffusion refiner significantly enhances generation quality and sharpness.

strategy allows us to obtain a smaller network while achieving performances comparable to those of the larger multiencoder VAE and retaining the same disentangled latent space.

**4.4.2 Training strategies.** We evaluate the semi-supervised training on model’s generation capabilities in Fig. 8. The base model (w/o semi-supervision) generates high-quality in-domain material but, as expected, struggles with out-domain materials absent from the original training data. The semi-supervised approach, in contrast, enhances diversity and overall quality, allowing the generation of materials beyond the initial training scope.

**4.4.3 High-resolution generation.** We evaluate our method with and without the refiner in Fig. 9. The generation looks sharper, less noisy, and more detailed. We demonstrate the effectiveness of our two-stage approach to high-resolution generation in Fig. 10, comparing it to patched diffusion, complemented by feature rolling. Patched diffusion leads to increased scale (pattern replication) rather than enhanced resolution (more pixel density) and causes inconsistencies like scale variations between patches. In contrast, our approach generates consistent and better quality high-res materials by refining

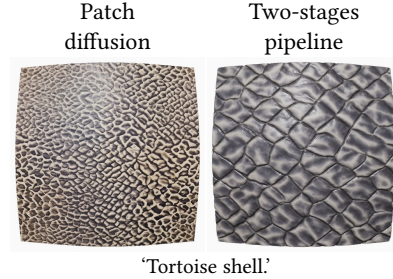


Fig. 10. **Ablation of the approaches to high-resolution.** (1) Patched diffusion produces more scale rather than resolution and presents inconsistency in scale. (2) Our two-stage approach generates at the model’s native resolution, and refines the material.



Fig. 11. **Limitations.** Left to right: (1) Struggles with complex prompts describing spatial relations. (2) Unable to represent complex figures or patterns. (3) Can hallucinate reflectance properties.

the generation at the model’s native resolution of  $512 \times 512$  pixels via a second diffusion step at the target resolution.

## 5 LIMITATIONS AND FUTURE WORK

StableMaterials presents some limitations as shown in Fig. 11. First, it struggles to handle natural prompts describing spatial relations and is unable to accurately represent complex concepts or figures. Introducing more variety in training prompts could help mitigate the problem. Additionally, it can occasionally generate incorrect reflectance properties (e.g.: material misclassified as metal) for material classes that are only present in the unannotated dataset. The use of text prompts describing surface properties, at training time, could mitigate the problem.

## 6 CONCLUSION

We present StableMaterials, a novel diffusion model for fast generation of tileable high-resolution materials. Our model leverages semi-supervised training and knowledge distillation from large-scale pre-trained models to overcome the limitations in training data and improve material realism and variety. This approach significantly reduces reliance on annotated data, thereby enriching the diversity and realism of generated PBR materials.

In conclusion, StableMaterials presents a robust solution to material generation challenges and we believe it can serve as a blueprint for future research to harness the potential of large-scale pretrained models and unsupervised data in computer graphics and beyond.

## REFERENCES

- Adobe. 2024. *Substance 3D Sampler (Beta) v4.4.1*. <https://www.adobe.com/it/products/substance3d-sampler.html>
- Martin Arjovsky, Soumith Chintala, and Léon Bottou. 2017. Wasserstein generative adversarial networks. In *International conference on machine learning*. PMLR, 214–223.
- Sai Bi, Zexiang Xu, Kalyan Sunkavalli, David Kriegman, and Ravi Ramamoorthi. 2020. Deep 3D Capture: Geometry and Reflectance from Sparse Multi-View Images. In *Proceedings of the IEEE/CVF Conference on Computer Vision and Pattern Recognition*. 5960–5969.
- Andrew Brock, Jeff Donahue, and Karen Simonyan. 2018. Large scale GAN training for high fidelity natural image synthesis. *arXiv preprint arXiv:1809.11096* (2018).
- Robert L Cook and Kenneth E. Torrance. 1982. A reflectance model for computer graphics. *ACM Transactions on Graphics (ToG)* 1, 1 (1982), 7–24.
- Valentin Deschaintre, Miika Aittala, Fredo Durand, George Drettakis, and Adrien Bousseau. 2018. Single-image svbrdf capture with a rendering-aware deep network. *ACM Transactions on Graphics (ToG)* 37, 4 (2018), 1–15.
- Valentin Deschaintre, Miika Aittala, Fredo Durand, George Drettakis, and Adrien Bousseau. 2019. Flexible SVBRDF Capture with a Multi-Image Deep Network. In *Computer Graphics Forum*, Vol. 38. Wiley Online Library, 1–13.
- Prafulla Dhariwal and Alexander Nichol. 2021. Diffusion models beat gans on image synthesis. *Advances in Neural Information Processing Systems* 34 (2021), 8780–8794.
- Alexey Dosovitskiy and Thomas Brox. 2016. Generating images with perceptual similarity metrics based on deep networks. *Advances in neural information processing systems* 29 (2016).
- Patrick Esser, Robin Rombach, and Bjorn Ommer. 2021. Taming transformers for high-resolution image synthesis. In *Proceedings of the IEEE/CVF conference on computer vision and pattern recognition*. 12873–12883.
- Duan Gao, Xiao Li, Yue Dong, Pieter Peers, Kun Xu, and Xin Tong. 2019. Deep inverse rendering for high-resolution SVBRDF estimation from an arbitrary number of images. *ACM Trans. Graph.* 38, 4 (2019), 134–1.
- Ian Goodfellow, Jean Pouget-Abadie, Mehdi Mirza, Bing Xu, David Warde-Farley, Sherjil Ozair, Aaron Courville, and Yoshua Bengio. 2014. Generative Adversarial Nets. In *Advances in Neural Information Processing Systems*, Z. Ghahramani, M. Welling, C. Cortes, N. Lawrence, and K.Q. Weinberger (Eds.), Vol. 27. Curran Associates, Inc. [https://proceedings.neurips.cc/paper\\_files/paper/2014/file/5ca3e9b122f61f8f06494c97b1afcc3-Paper.pdf](https://proceedings.neurips.cc/paper_files/paper/2014/file/5ca3e9b122f61f8f06494c97b1afcc3-Paper.pdf)
- Darya Guarnera, Giuseppe Claudio Guarnera, Abhijeet Ghosh, Cornelia Denz, and Mashhuda Glencross. 2016. BRDF representation and acquisition. In *Computer Graphics Forum*, Vol. 35. Wiley Online Library, 625–650.
- Pascal Guehl, Rémi Allegre, J-M Dischler, Bedrich Benes, and Eric Galin. 2020. Semi-Procedural Textures Using Point Process Texture Basis Functions. In *Computer Graphics Forum*, Vol. 39. Wiley Online Library, 159–171.
- Ishaan Gulrajani, Faruk Ahmed, Martin Arjovsky, Vincent Dumoulin, and Aaron C Courville. 2017. Improved training of wasserstein gans. *Advances in neural information processing systems* 30 (2017).
- Jie Guo, Shuichang Lai, Chengzhi Tao, Yuelong Cai, Lei Wang, Yanwen Guo, and Ling-Qi Yan. 2021. Highlight-aware two-stream network for single-image SVBRDF acquisition. *ACM Transactions on Graphics (TOG)* 40, 4 (2021), 1–14.
- Yu Guo, Cameron Smith, Miloš Hašan, Kalyan Sunkavalli, and Shuang Zhao. 2020. MaterialGAN: reflectance capture using a generative svbrdf model. *arXiv preprint arXiv:2010.00114* (2020).
- Zhen He, Jie Guo, Yan Zhang, Qinghao Tu, Mufan Chen, Yanwen Guo, Pengyu Wang, and Wei Dai. 2023. Text2Mat: Generating Materials from Text. In *Pacific Graphics Short Papers and Posters*, Raphaëlle Chaine, Zhigang Deng, and Min H. Kim (Eds.). The Eurographics Association. <https://doi.org/10.2312/pg.20231275>
- Jonathan Ho, Ajay Jain, and Pieter Abbeel. 2020. Denoising diffusion probabilistic models. *Advances in Neural Information Processing Systems* 33 (2020), 6840–6851.
- Edward J Hu, Yelong Shen, Phillip Wallis, Zeyuan Allen-Zhu, Yuanzhi Li, Shean Wang, Lu Wang, and Weizhu Chen. 2021. Lora: Low-rank adaptation of large language models. *arXiv preprint arXiv:2106.09685* (2021).
- Yiwei Hu, Miloš Hašan, Paul Guerrero, Holly Rushmeier, and Valentin Deschaintre. 2022. Controlling Material Appearance by Examples. In *Computer Graphics Forum*, Vol. 41. Wiley Online Library, 117–128.
- Phillip Isola, Jun-Yan Zhu, Tinghui Zhou, and Alexei A Efros. 2017. Image-to-image translation with conditional adversarial networks. In *Proceedings of the IEEE conference on computer vision and pattern recognition*. 1125–1134.
- Brian Karis. 2013. Real shading in unreal engine 4. *Proc. Physically Based Shading Theory Practice* 4, 3 (2013), 1.
- Tero Karras, Timo Aila, Samuli Laine, and Jaakko Lehtinen. 2017. Progressive growing of gans for improved quality, stability, and variation. *arXiv preprint arXiv:1710.10196* (2017).
- Tero Karras, Samuli Laine, Miika Aittala, Janne Hellsten, Jaakko Lehtinen, and Timo Aila. 2020a. Analyzing and improving the image quality of stylegan. In *Proceedings of the IEEE/CVF conference on computer vision and pattern recognition*. 8110–8119.
- Tero Karras, Samuli Laine, Miika Aittala, Janne Hellsten, Jaakko Lehtinen, and Timo Aila. 2020b. Analyzing and improving the image quality of stylegan. In *Proceedings of the IEEE/CVF conference on computer vision and pattern recognition*. 8110–8119.
- Diederik P Kingma and Jimmy Ba. 2014. Adam: A method for stochastic optimization. *arXiv preprint arXiv:1412.6980* (2014).
- Diederik P Kingma and Max Welling. 2013. Auto-encoding variational bayes. *arXiv preprint arXiv:1312.6114* (2013).
- Xiao Li, Yue Dong, Pieter Peers, and Xin Tong. 2017. Modeling surface appearance from a single photograph using self-augmented convolutional neural networks. *ACM Transactions on Graphics (ToG)* 36, 4 (2017), 1–11.
- Zhengqin Li, Kalyan Sunkavalli, and Manmohan Chandraker. 2018. Materials for masses: SVBRDF acquisition with a single mobile phone image. In *Proceedings of the European Conference on Computer Vision (ECCV)*. 72–87.
- Jae Hyun Lim and Jong Chul Ye. 2017. Geometric gan. *arXiv preprint arXiv:1705.02894* (2017).
- Ivan Lopes, Fabio Pizzati, and Raoul de Charette. 2024. Material Palette: Extraction of Materials from a Single Image. In *Proceedings of the IEEE/CVF Conference on Computer Vision and Pattern Recognition*.
- Ilya Loshchilov and Frank Hutter. 2017. Decoupled weight decay regularization. *arXiv preprint arXiv:1711.05101* (2017).
- Simian Luo, Yiqin Tan, Longbo Huang, Jian Li, and Hang Zhao. 2023. Latent consistency models: Synthesizing high-resolution images with few-step inference. *arXiv preprint arXiv:2310.04378* (2023).
- Weijian Luo, Tianyang Hu, Shifeng Zhang, Jiacheng Sun, Zhenguo Li, and Zhihua Zhang. 2024. Diff-instruct: A universal approach for transferring knowledge from pre-trained diffusion models. *Advances in Neural Information Processing Systems* 36 (2024).
- Xiaohu Ma, Xianmin Xu, Leyao Zhang, Kun Zhou, and Hongzhi Wu. 2023. OpenSVBRDF: A Database of Measured Spatially-Varying Reflectance. *ACM Transactions on Graphics (TOG)* 42, 6 (2023), 1–14.
- Rosalie Martin, Arthur Roullier, Romain Rouffet, Adrien Kaiser, and Tamy Boubekeur. 2022. MaterIA: Single Image High-Resolution Material Capture in the Wild. In *Computer Graphics Forum*, Vol. 41. Wiley Online Library, 163–177.
- Chenlin Meng, Yutong He, Yang Song, Jiaming Song, Jiajun Wu, Jun-Yan Zhu, and Stefano Ermon. 2021. Sdedit: Guided image synthesis and editing with stochastic differential equations. *arXiv preprint arXiv:2108.01073* (2021).
- Chenlin Meng, Robin Rombach, Ruiqi Gao, Diederik Kingma, Stefano Ermon, Jonathan Ho, and Tim Salimans. 2023. On distillation of guided diffusion models. In *Proceedings of the IEEE/CVF Conference on Computer Vision and Pattern Recognition*. 14297–14306.
- Lars Mescheder. 2018. On the convergence properties of gan training. *arXiv preprint arXiv:1801.04406* 1 (2018), 16.
- OpenAI. 2024. *ChatGPT*. <https://chatgpt.com/>
- Dustin Podell, Zion English, Kyle Lacey, Andreas Blattmann, Tim Dockhorn, Jonas Müller, Joe Penna, and Robin Rombach. 2023. Sdxl: Improving latent diffusion models for high-resolution image synthesis. *arXiv preprint arXiv:2307.01952* (2023).
- Alec Radford, Jong Wook Kim, Chris Hallacy, Aditya Ramesh, Gabriel Goh, Sandhini Agarwal, Girish Sastry, Amanda Askell, Pamela Mishkin, Jack Clark, et al. 2021. Learning transferable visual models from natural language supervision. In *International conference on machine learning*. PMLR, 8748–8763.
- Danilo Jimenez Rezende, Shakir Mohamed, and Daan Wierstra. 2014. Stochastic back-propagation and approximate inference in deep generative models. In *International conference on machine learning*. PMLR, 1278–1286.
- Robin Rombach, Andreas Blattmann, Dominik Lorenz, Patrick Esser, and Björn Ommer. 2022. High-resolution image synthesis with latent diffusion models. In *Proceedings of the IEEE/CVF conference on computer vision and pattern recognition*. 10684–10695.
- Olaf Ronneberger, Philipp Fischer, and Thomas Brox. 2015. U-net: Convolutional networks for biomedical image segmentation. In *International Conference on Medical image computing and computer-assisted intervention*. Springer, 234–241.
- Nataniel Ruiz, Yuanzhen Li, Varun Jampani, Yael Pritch, Michael Rubinstein, and Kfir Aberman. 2023. Dreambooth: Fine tuning text-to-image diffusion models for subject-driven generation. In *Proceedings of the IEEE/CVF Conference on Computer Vision and Pattern Recognition*. 22500–22510.
- Axel Sauer, Frederic Boesel, Tim Dockhorn, Andreas Blattmann, Patrick Esser, and Robin Rombach. 2024. Fast High-Resolution Image Synthesis with Latent Adversarial Diffusion Distillation. *arXiv preprint arXiv:2403.12015* (2024).
- Axel Sauer, Kashyap Chitta, Jens Müller, and Andreas Geiger. 2021. Projected gans converge faster. *Advances in Neural Information Processing Systems* 34 (2021), 17480–17492.
- Axel Sauer, Tero Karras, Samuli Laine, Andreas Geiger, and Timo Aila. 2023a. Stylegan-t: Unlocking the power of gans for fast large-scale text-to-image synthesis. In *International conference on machine learning*. PMLR, 30105–30118.
- Axel Sauer, Dominik Lorenz, Andreas Blattmann, and Robin Rombach. 2023b. Adversarial diffusion distillation. *arXiv preprint arXiv:2311.17042* (2023).
- Christoph Schuhmann, Romain Beaumont, Richard Vencu, Cade Gordon, Ross Wightman, Mehdi Cherti, Theo Coombes, Arush Katta, Clayton Mullis, Mitchell Wortsman, et al. 2022. Laion-5b: An open large-scale dataset for training next generation



- image-text models. *Advances in Neural Information Processing Systems* 35 (2022), 25278–25294.
- Jascha Sohl-Dickstein, Eric Weiss, Niru Maheswaranathan, and Surya Ganguli. 2015. Deep unsupervised learning using nonequilibrium thermodynamics. In *International Conference on Machine Learning*. PMLR, 2256–2265.
- Yang Song, Prafulla Dhariwal, Mark Chen, and Ilya Sutskever. 2023. Consistency models. *arXiv preprint arXiv:2303.01469* (2023).
- Giuseppe Vecchio and Valentin Deschaintre. 2024. MatSynth: A Modern PBR Materials Dataset. In *Proceedings of the IEEE/CVF Conference on Computer Vision and Pattern Recognition*.
- Giuseppe Vecchio, Rosalie Martin, Arthur Roullier, Adrien Kaiser, Romain Rouffet, Valentin Deschaintre, and Tamy Boubekeur. 2023. ControlMat: Controlled Generative Approach to Material Capture. *arXiv preprint arXiv:2309.01700* (2023).
- Giuseppe Vecchio, Simone Palazzo, and Concetto Spampinato. 2021. SurfaceNet: Adversarial svbrdf estimation from a single image. In *Proceedings of the IEEE/CVF International Conference on Computer Vision*. 12840–12848.
- Giuseppe Vecchio, Renato Sortino, Simone Palazzo, and Concetto Spampinato. 2024. MatFuse: Controllable Material Generation with Diffusion Models. In *Proceedings of the IEEE/CVF Conference on Computer Vision and Pattern Recognition*.
- Bruce Walter, Stephen R Marschner, Hongsong Li, and Kenneth E Torrance. 2007. Microfacet models for refraction through rough surfaces. In *Proceedings of the 18th Eurographics conference on Rendering Techniques*. 195–206.
- Kai Zhang, Jingyun Liang, Luc Van Gool, and Radu Timofte. 2021. Designing a practical degradation model for deep blind image super-resolution. In *Proceedings of the IEEE/CVF International Conference on Computer Vision*. 4791–4800.
- Xilong Zhou, Milos Hasan, Valentin Deschaintre, Paul Guerrero, Kalyan Sunkavalli, and Nima Khademi Kalantari. 2022. TileGen: Tileable, Controllable Material Generation and Capture. In *SIGGRAPH Asia 2022 Conference Papers*. 1–9.
- Xilong Zhou, Miloš Hašan, Valentin Deschaintre, Paul Guerrero, Yannick Hold-Geoffroy, Kalyan Sunkavalli, and Nima Khademi Kalantari. 2023. PhotoMat: A Material Generator Learned from Single Flash Photos. In *SIGGRAPH 2023 Conference Papers*.
- Xilong Zhou and Nima Khademi Kalantari. 2021. Adversarial Single-Image SVBRDF Estimation with Hybrid Training. In *Computer Graphics Forum*, Vol. 40. Wiley Online Library, 315–325.

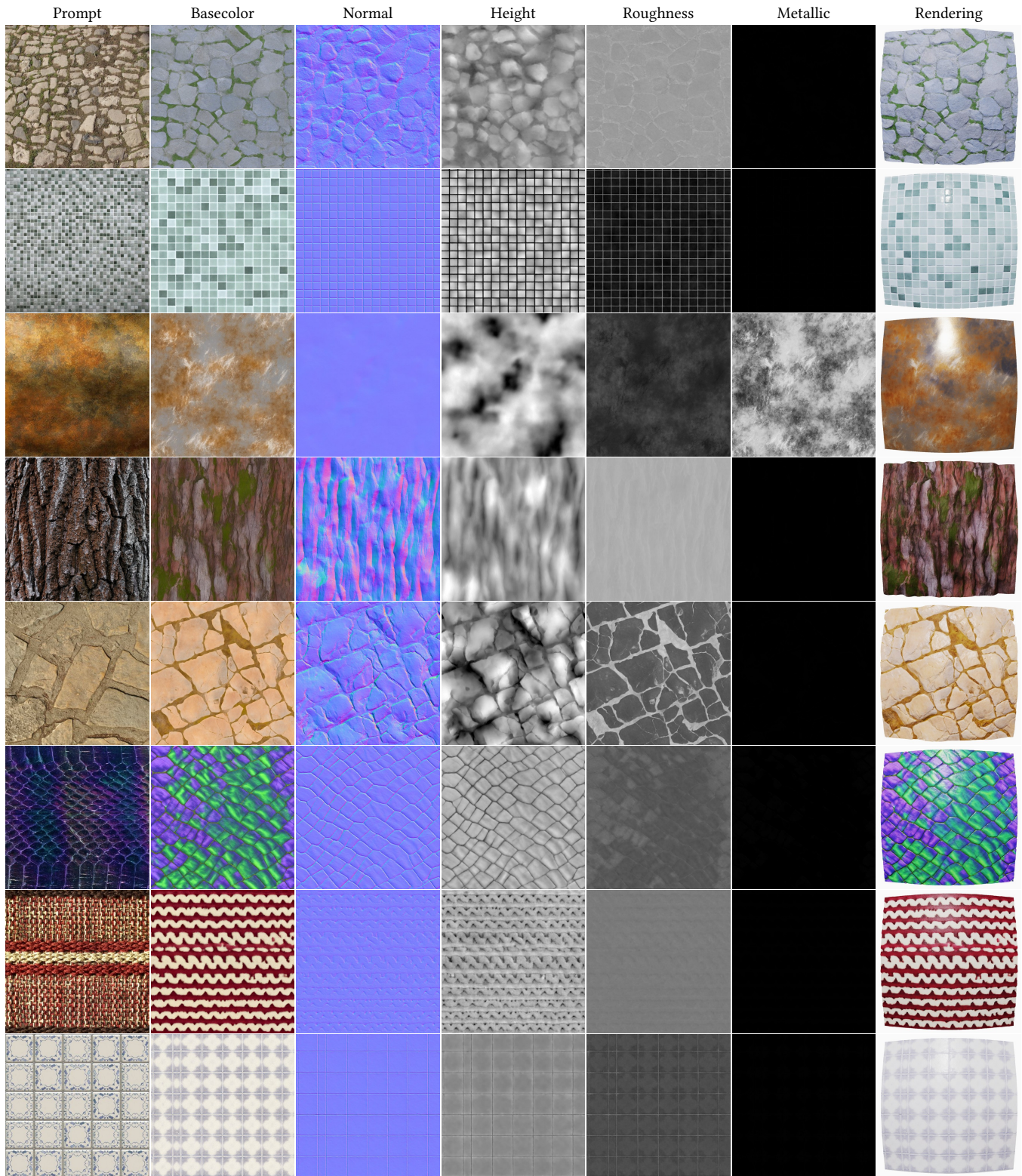


Fig. 12. **Image-prompting.** We show here a variety of materials generate using image prompts. StableMaterials is able to capture the visual feature of each input condition and generate a new, visually similar, material. Additional results are included in the Supplemental material.

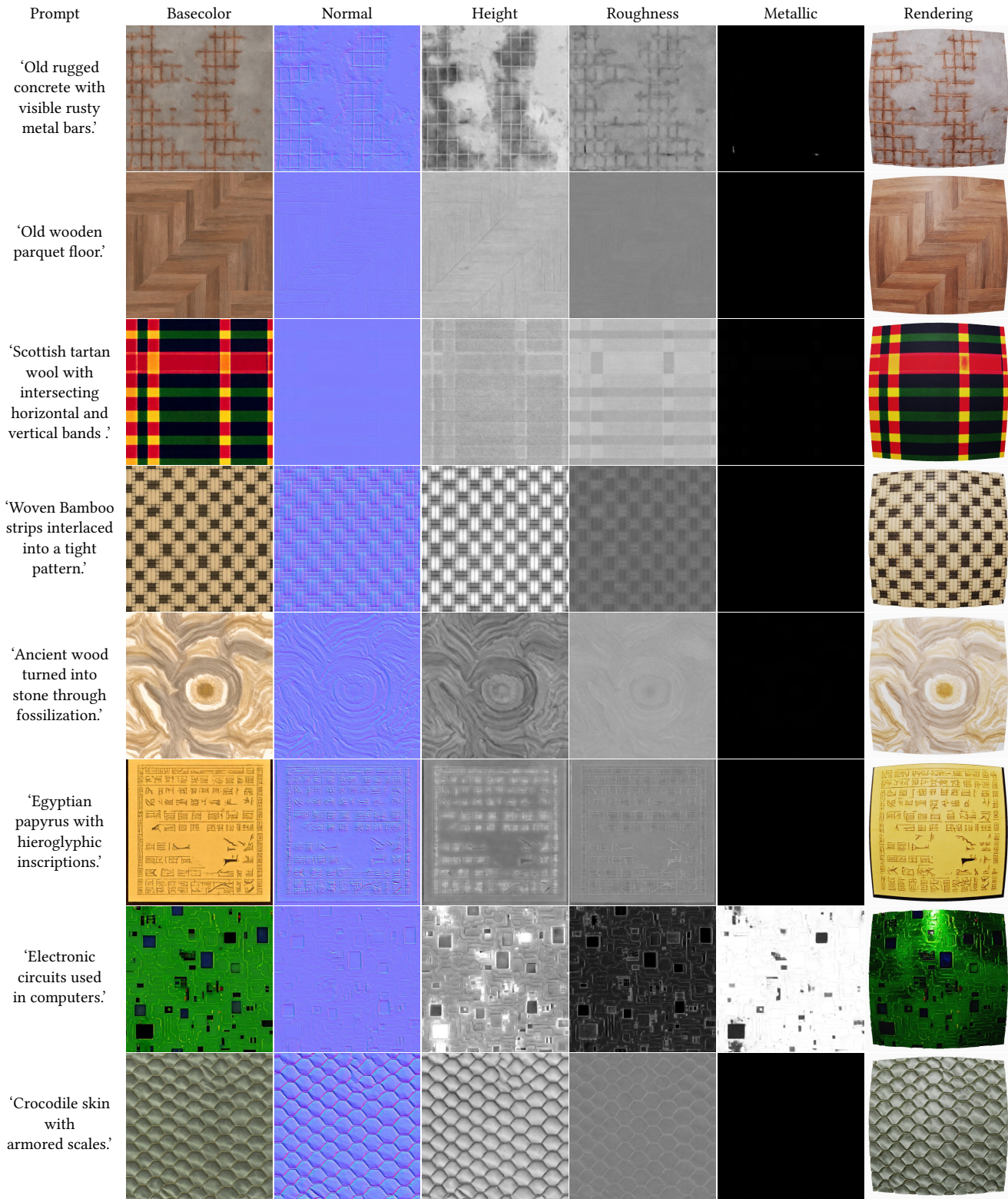


Fig. 13. **Text-prompting.** We show here a variety of materials generate using text prompts. StableMaterials is able to generate a new material representing the features described in the input prompt. Additional results are included in the Supplemental material.